Original Article

Artificial intelligence-driven quantitative analysis of CT morphological differences between chronic thromboembolic pulmonary hypertension and chronic thromboembolic disease

Wenqing Xu[1]^, Linfeng Xi[2], Yifei Ni[3], Jianping Wang[4], Haoyu Yang[5], Anqi Liu[3], Qian Gao[2], Xincao Tao[2], Qiang Huang[2], Xiaopeng Liu[6], Yanan Zhen[6], Wanmu Xie[2], Min Liu[7]

[1]Department of Magnetic Resonance Imaging, Fuwai Hospital and National Center for Cardiovascular Diseases, Chinese Academy of Medical Sciences and Peking Union Medical College, Beijing, China; [2]Department of Pulmonary and Critical Care Medicine, Center of Respiratory Medicine, China-Japan Friendship Hospital National Center for Respiratory Medicine, Beijing, China; [3]Department of Radiology, China-Japan Friendship Hospital, Chinese Academy of Medical Sciences & Peking Union Medical College, Beijing, China; [4]Department of Radiology, China-Japan Friendship Hospital, Capital Medical University, Beijing, China; [5]Peking University China-Japan Friendship School of Clinical Medicine, Beijing, China; [6]Department of Cardiovascular Surgery, China-Japan Friendship Hospital, Beijing, China; [7]Department of Radiology, China-Japan Friendship Hospital, Beijing, China

Contributions: (I) Conception and design: W Xu, M Liu; (II) Administrative support: M Liu; (III) Provision of study materials or patients: W Xu, L Xi, Y Ni, J Wang; (IV) Collection and assembly of data: W Xu, L Xi, X Tao, H Yang; (V) Data analysis and interpretation: W Xu, L Xi, A Liu; (VI) Manuscript writing: All authors; (VII) Final approval of manuscript: All authors.

Correspondence to: Min Liu, MD. Department of Radiology, China-Japan Friendship Hospital, No. 2 Yinghua Dong Street, Hepingli, Chaoyang District, Beijing 100029, China. Email: mikie0763@126.com.

Background: The morphological differences in the pulmonary vascular tree between chronic thromboembolic pulmonary hypertension (CTEPH) and chronic thromboembolic disease (CTED) are not yet fully understood. This study aimed to use artificial intelligence (AI) segmentation technology to identify morphological markers that can be used to differentiate CTEPH from CTED using computed tomography pulmonary angiography (CTPA).

Methods: We conducted a retrospective cohort study with consecutive patients diagnosed with CTEPH, CTED, and control subjects at the China-Japan Friendship Hospital from January 2019 to October 2023. The study involved the automatic quantification of the pulmonary blood volume (BV), tortuosity, and fractal dimension (FD) from CTPA images using an AI workstation. These morphological metrics were compared among the three groups using the Kruskal-Wallis test. Correlations between these metrics and the hemodynamic parameters were evaluated using Spearman's rank correlation coefficients. Additionally, a receiver operating characteristic (ROC) curve analysis was conducted to assess the discriminative ability of pulmonary artery tortuosity to differentiate between each pair of groups.

Results: A total of 190 participants [57 years, interquartile range (IQR), 49–65 years, 97 men], including 116 CTEPH patients, 54 CTED patients, and 20 controls, were enrolled in this study. Pulmonary artery tortuosity in the control, CTED, and CTEPH groups showed a progressively increasing trend [1.07 (IQR, 1.06–1.10) *vs.* 1.10 (IQR, 1.07–1.14) *vs.* 1.14 (IQR, 1.10–1.18), P<0.01]. The area under the curve (AUC) values of pulmonary arterial tortuosity for differentiating between the CTEPH patients and controls, CTED patients and controls, and CTEPH patients and CTED patients were 0.859, 0.712, and 0.663, respectively. There was a positive correlation between pulmonary artery tortuosity and mean pulmonary arterial pressure (mPAP) (r=0.44, P<0.01), and pulmonary vascular resistance (PVR) (r=0.47, P<0.01). Additionally, the

^ ORCID: 0000-0001-8199-9693.

volume of the small- and medium-sized pulmonary arteries was significantly higher in the CTED patients than the CTEPH patients (P<0.01). The pulmonary arterial FD among the three groups was comparable (P=0.36).

Conclusions: Pulmonary arterial tortuosity on CTPA had auxiliary diagnostic value in differentiating between CTEPH patients and controls, but its value in differentiating between CTED and CTEPH patients requires further study. The reduced volume of small- and medium-sized pulmonary arteries in CTEPH patients could indicate impaired pulmonary hemodynamics.

Keywords: Chronic thromboembolic pulmonary hypertension (CTEPH); chronic thromboembolic pulmonary disease; computed tomography (CT); artificial intelligence (AI); tortuosity

Submitted Jun 27, 2024. Accepted for publication Dec 19, 2024. Published online Jan 22, 2025.
doi: 10.21037/qims-24-1301
View this article at: https://dx.doi.org/10.21037/qims-24-1301

Introduction

Chronic thromboembolic pulmonary hypertension (CTEPH) and chronic thromboembolic disease (CTED) share similarities in terms of etiology, symptoms, and vascular damage (1); however, they differ in terms of pulmonary vascular pathology (2-6). Currently, there is no evidence that CTED inevitably progresses to CTEPH (7). CTEPH is characterized by more extensive vascular obstruction than CTED, primarily at the segmental level; thus, vascular obstruction is a dominant feature in its pathophysiology (8). The 2022 European guidelines highlight the importance of evaluating CTED to minimize the risks of misdiagnosis and missed diagnoses (4).

Computed tomography pulmonary angiography (CTPA) provides important findings of pulmonary embolism and pulmonary hypertension (PH). Recent advances in image analysis, particularly those involving artificial intelligence (AI), have enabled the automatic segmentation and quantification of pulmonary arteries, veins, and airway structures (9,10). These innovations enhance the assessment of pulmonary diseases such as PH, pulmonary fibrosis, and chronic obstructive pulmonary disease (10-14). Morphological parameters, such as volume, tortuosity, and fractal dimension (FD), can be automatically quantified on computed tomography (CT), offering novel insights into the evaluation of pulmonary vessels and airways (9,10,12,13). However, these new parameters are rarely used to evaluate diseases associated with pulmonary embolism, and their hemodynamic effects.

This study sought to employ an AI-based algorithm to quantitatively analyze differences in morphological parameters on CTPA between CTEPH and CTED. It also aimed to explore the correlation between these morphological parameters and both hemodynamic and clinical markers. We present this article in accordance with the STROBE reporting checklist (available at https://qims.amegroups.com/article/view/10.21037/qims-24-1301/rc).

Methods

Population and study design

This single-center study was approved by the China-Japan Friendship Hospital's Ethics Committee (No. 2022-KY-048) and conducted in accordance with the Declaration of Helsinki (as revised in 2013). The requirement of informed consent was waived due to the retrospective nature of the study. Patients who underwent right heart catheterization (RHC) for suspected CTEPH at China-Japan Friendship Hospital between January 2019 and October 2023 were retrospectively enrolled in this study if they underwent both CTPA and RHC within 2 weeks. Both CTEPH and CTED were diagnosed based on findings from either CTPA or ventilation/perfusion (V/Q) scans. The diagnostic criteria for chronic thromboembolism were as follows (4): after a minimum of 3 months of standardized anticoagulation therapy, the presence of chronic thrombosis was confirmed by either CTPA or V/Q scans. Specifically, the V/Q scan had to reveal perfusion defects involving two or more segments that did not match ventilation abnormalities, or the CTPA scan had to reveal signs of chronic thromboembolism. Patients in the CTEPH group were required to have a resting mean pulmonary arterial pressure (mPAP) >20 mmHg, and pulmonary vascular resistance (PVR)

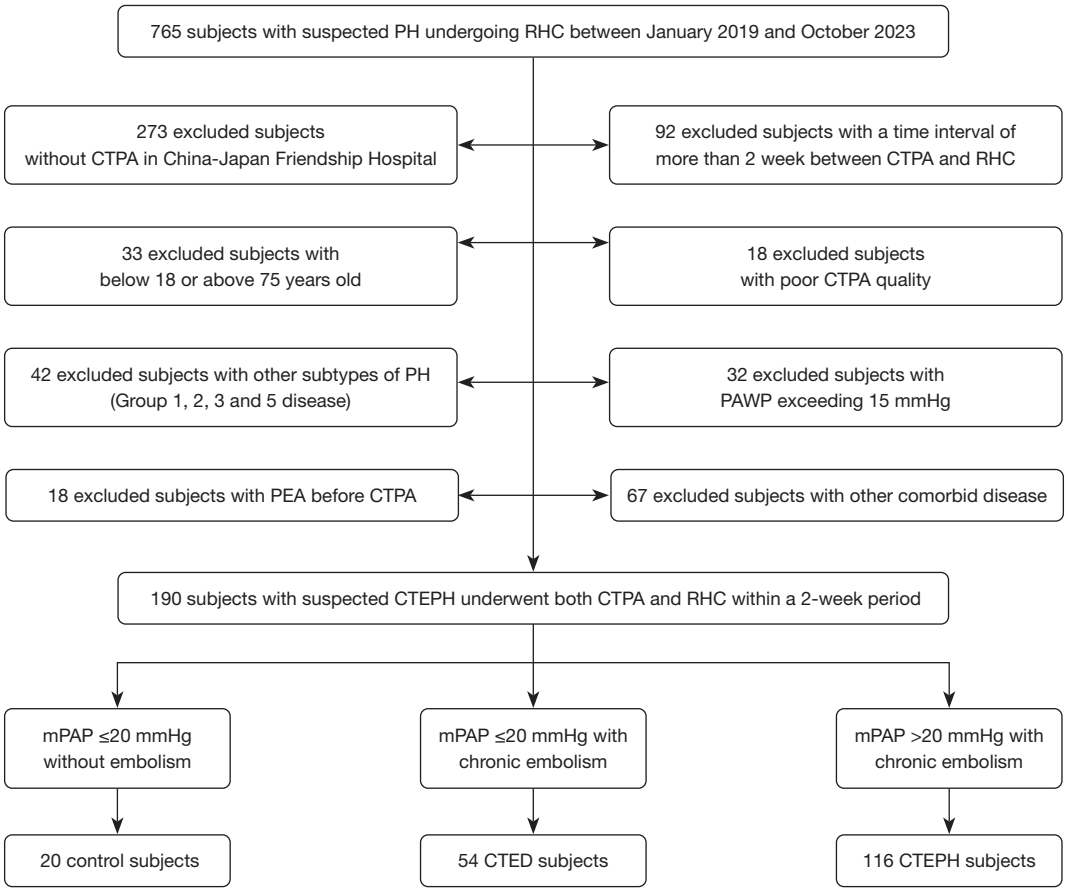

Figure 1 Flow chart detailing selection of participant cohorts. PH, pulmonary hypertension; RHC, right heart catheterization; CTPA, computed tomography pulmonary angiography; PEA, pulmonary endarterectomy; PAWP, pulmonary artery wedge pressure; CTEPH, chronic thromboembolic pulmonary hypertension; mPAP, mean pulmonary arterial pressure; CTED, chronic thromboembolic disease.

>2 Wood units (WU). Patients with an mPAP <20 mmHg were further categorized into two groups: the CTED group, which comprised patients with chronic pulmonary embolism, and the control group, which comprised patients without chronic pulmonary embolism.

Patients were excluded from the study if they met any of the following exclusion criteria: (I) were aged <18 or >75 years; (II) had not undergone CTPA or RHC at China-Japan Friendship Hospital; (III) had poor-quality CTPA images (e.g., motion artifacts or inadequate contrast enhancement), or incomplete RHC data; (IV) had been diagnosed with fibrosing mediastinitis, vasculitis, or pulmonary artery sarcoma; (V) had other subtypes of PH (Group 1, 2, 3, or 5); (VI) had pulmonary artery wedge pressure (PAWP) >15 mmHg or mPAP >20 mmHg but low PVR (≤2 WU); (VII) had congenital heart disease; and/or (VIII) had undergone pulmonary thromboendarterectomy prior to CTPA. *Figure 1* provides a flowchart outlining the participant selection process and group allocation.

CTPA scan protocol

All patients underwent supine CTPA with either a 256-row CT (GE Revolution CT, USA) or a 320-row CT (Aquilion ONE, Japan) at the end of expiration, from the lung base to the apex. For the GE Revolution CT, the CTPA scan parameters were as follows: tube rotation speed: 0.28 s/rotation; tube voltage: kilovolt intelligent decision technology (kilovolt assist; 100 and 120 kV); pitch: 0.992:1; slices × collimator width: 256 × 0.625 mm; and reconstruction image slice thickness and spacing: 0.625 mm. For the Aquilion ONE, the CTPA scan parameters were as follows: tube rotation speed: 0.35 s/rotation; tube voltage: 120 kVp; slices × collimator width: 320 × 0.5 mm;

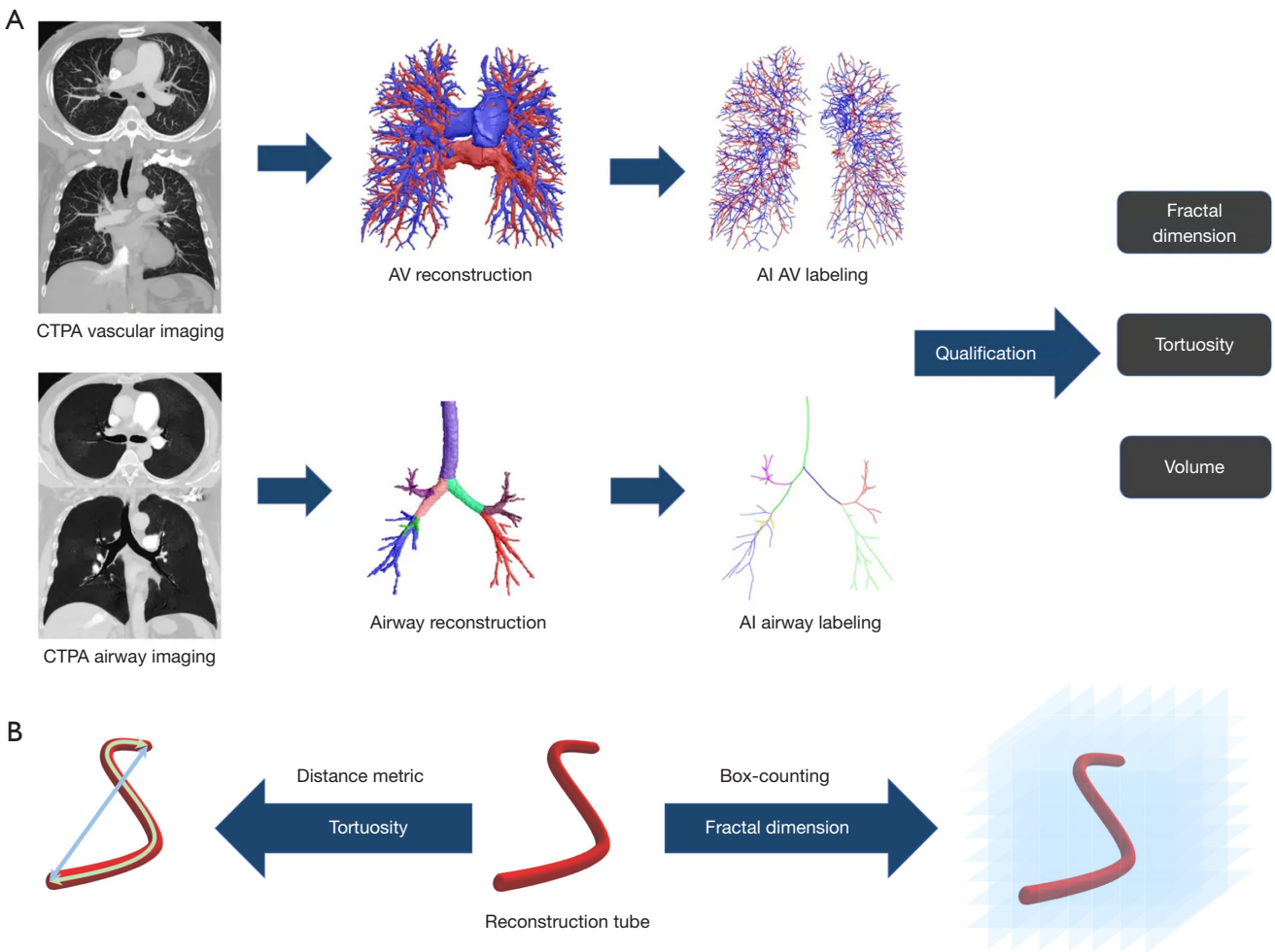

Figure 2 Measurement of vessel and airway parameters on three-dimensional in-home AI workstation. (A) Vessel and airway reconstruction, segmentation, skeleton extraction, and qualification; pulmonary arteries are shown in blue, and veins are shown in red. (B) Schematic diagram of tortuosity and fractal dimension calculation. CTPA, computed tomography pulmonary angiography; AV, arteriovenous; AI, artificial intelligence.

and reconstruction image slice thickness and spacing: 0.5 mm. The non-ionic contrast agent was Ultravist (370 mg I/mL, Schering Bayer), and the injection speed was 4 to 4.5 mL/s and 50 mL of physiological saline was used. The contrast agent detection method was automatically triggered, with the main pulmonary artery level selected as the trigger point, and the trigger threshold was set at 80 HU.

Quantification of pulmonary vessel and airway parameters

CTPA images in Digital Imaging and Communications in Medicine (DICOM) format were transferred to a three-dimensional, in-house AI workstation (FACT AI+digitalLung version 1.0, Shenzhou Dexin Medical Imaging Technology Co., Ltd., Shanxi, China, http://www.dexhin.com). Pulmonary vessels and airway trees were automatically segmented using a deep learning-based algorithm (15,16) (*Figure 2A*). A schematic diagram illustrating the method for calculating the tortuosity and FD of the pulmonary vascular tree is shown in *Figure 2B*. The detailed steps for segmentation, bone extraction, and the measurement of tortuosity and FD have been described in previous research (9).

The calculation of tortuosity followed the distance metric technique described in earlier studies (10,13). Tortuosity was defined as the ratio of the actual length of a vessel segment (between the bifurcation points or terminal ends) to the straight-line distance between those same points. Additionally, given the parallel anatomical characteristic of the pulmonary arteries and airways, we introduced a novel metric; that is, the bronchovascular bundle tortuosity difference, which measures the tortuosity difference between the pulmonary artery and the airway.

The FD of pulmonary vessels and airways was calculated using the box-counting method to assess the complexity and space-filling nature of these tubular structures (11,13,14).

Pulmonary BV-related metrics were also automatically segmented and quantified, including the total volume of vessels, total blood volume of pulmonary arteries (TBV_{ART}), total blood volume of pulmonary veins (TBV_{VEIN}), number of vessel branches, and cross-sectional area of these vessels. To classify the vascular blood volume (BV), we categorized vessels into the following three groups based on their cross-sectional areas (10,17): BV5, BV10, and BV10+, representing vessels with cross-sectional areas <5 mm^2, <10 mm^2, and >10 mm^2, respectively. To ensure comparability and accuracy in comparisons between different groups, the following two standardization methods were employed for processing (13): (I) the proportions of BV5, BV10, and BV10+ relative to the total lung volume were expressed as ρBV5, ρBV10, and ρBV10+, respectively; (II) the proportions of these metrics relative to the total blood volume (TBV) in the area of interest were represented as BV5/TBV, BV10/TBV, and BV10+/TBV, respectively.

In addition, conventional metrics were independently measured on CTPA axial images by two experienced chest radiologists (with 6 years of experience each). These included the main pulmonary artery diameter (MPAd), the ascending aorta diameter (AAd), and the maximum transverse diameters of the right ventricle and left ventricle ratio (RV/LV ratio).

RHC

All participants received RHC via the right internal jugular or the femoral vein using a 6F Swan-Ganz device (Bioptimal, for Thermodilution). The following resting hemodynamic parameters were recorded: mPAP, PAWP, mean right atrial pressure (mRAP), and stroke volume (SV), as well as the cardiac output (CO) and cardiac index (CI) during this process. PVR was calculated using the following formula (18): PVR (WU) = (mPAP – PAWP)/CO.

Statistical analysis

The statistical analysis was performed using IBM SPSS Statistics 27.0 (SPSS Inc., for MAC, IBM Corp., Armonk, USA), Graphpad Prism (version 9.5.0, GraphPad Software, USA), and Origin (version 2021, OriginLab Corporation, USA). The Shapiro-Wilks test was used to assess the normality of the variables. The continuous variables are expressed as the median value with the interquartile range (IQR). The normally distributed variables were subjected to between-group comparisons using a one-way analysis of variance, with subsequent *post-hoc* pairwise analyses of significant variances applying Bonferroni adjustments for multiple comparisons. For the non-parametric multiple-group comparisons, the Kruskal-Wallis test was used. The count data are expressed as the frequency (percentage), and were analyzed for statistical differences using the chi-square test or Fisher's exact test. A receiver operating characteristic (ROC) curve analysis was conducted to examine pulmonary arteries tortuosity and the bronchovascular bundle tortuosity difference. The correlations between the CTPA morphologic parameters, hemodynamics, and clinic data were analyzed using Spearman's rank correlation coefficients. The classification of correlation coefficients was as follows: $r<0.2$: no correlation; $0.2\leq r<0.4$: weak correlation; $0.4\leq r<0.6$: moderate correlation; $0.6\leq r<0.8$: strong correlation; and $r\geq 0.8$: very strong correlation. Two-sided P values of <0.05 were considered statistically significant.

Results

Patient characteristics

The study ultimately enrolled 190 patients (57 years, IQR, 49–65 years, 97 men), comprising 116 CTEPH patients (59 years, IQR, 51–66 years, 58 men), 54 CTED patients (54 years, IQR, 45–66 years, 29 men), and 20 control subjects (54 years, IQR, 48–61 years, 9 men). As *Figure 1* shows, CTPA images from 18 patients were excluded due to unsuccessful vessel or airway segmentation on the AI workstation, resulting in a segmentation success rate of 92%. The post-processing time for each CTPA dataset was approximately 3–5 minutes per patient. *Table 1* presents the demographic and clinical data, while intergroup comparisons are detailed in Table S1. The CTED and

Table 1 Demographic and clinical characteristics and hemodynamics of patients in the CTED, CTEPH, and control groups

Characteristics	Control group (N=20)	CTED group (N=54)	CTEPH group (N=116)	P value[a]
Age (years)	54 [48–61]	54 [45–66]	59 [51–66]	0.12
Gender (male/female)	9/11	29/25	58/58	0.92
BMI (kg/m^2)	24 [19–28]	25 [23–27]	24 [22–27]	0.41
NT-proBNP (pg/mL)	43 [16–68]	54 [24–83]	453 [121–1,241]	<0.01
6MWD (m)	497 [461–516]	482 [450–554]	392 [300–460]	<0.01
NYHA FC (III/IV)	0	6 (11.1)	54 (46.5)	<0.01
Resting supine hemodynamics				
mPAP (mmHg)	14 [10–16]	16 [13–18]	39 [29–47]	<0.01
PAWP (mmHg)	8 [5–12]	10 [8–12]	10 [8–12]	0.30
PVR (WU)	1.3 [0.6–1.6]	1.4 [0.8–1.9]	9.1 [5.6–13.6]	<0.01
SV (mL)	64.4 [52.3–85.3]	63.0 [51.8–77.8]	47.8 [32.9–61.1]	<0.01
CO (L/min)	4.4 [4.2–5.1]	4.6 [3.8–5.3]	3.4 [2.5–4.2]	<0.01
CI (L/min/m^2)	2.7 [2.3–2.9]	2.5 [2.2–3.2]	2.0 [1.6–2.3]	<0.01

The data are reported as the median [interquartile range] for the continuous variables, and the number (percentage) for the count data. [a], P value represents two-sided significance from a one-way analysis of variance, Shapiro-Wilks test, chi-square test, or Fisher's exact test. CTED, chronic thromboembolic disease; CTEPH, chronic thromboembolic pulmonary hypertension; BMI, body mass index; NT-proBNP, N-terminal-pro-B-type natriuretic peptide; 6MWD, 6-minute walking distance; NYHA FC, New York Heart Association classification functional class; mPAP, mean pulmonary arterial pressure; PAWP, pulmonary artery wedge pressure; PVR, pulmonary vascular resistance; WU, Wood units; SV, stroke volume; CO, cardiac output; CI, cardiac index.

control groups had significantly lower mPAP and PVR than the CTEPH patients (P<0.01).

Pulmonary morphological parameters

Figure 3 presents cases of pulmonary vascular morphology in CTEPH and CTED patients. *Table 2* summarizes the tortuosity and FD of pulmonary arteries, veins, and airways, with detailed intergroup comparisons presented in Table S2. The pulmonary artery tortuosity and bronchovascular bundle tortuosity difference exhibited a stepwise increase, rising from the control group to the CTED group, and rising further to the CTEPH group (P<0.01). However, the FD of the pulmonary arteries did not differ significantly among the three groups (P=0.36). Similarly, both the tortuosity (P=0.50) and FD (P=0.23) of the pulmonary veins were comparable across the three groups.

As *Table 3* shows, the small- and medium-sized pulmonary artery volume parameters, such as ρBV5, ρBV10, BV5/TBV_{ART}, and BV10/TBV_{ART}, were lower in the CTEPH group than the CTED group. Conversely, as *Figure 4* shows, the large pulmonary artery volume parameters, such as ρBV10+ and BV10+/TBV_{ART}, were higher in the CTEPH group (P<0.01). No significant differences were observed in the standardized venous parameters between the CTEPH and CTED groups. Intergroup comparisons are detailed in Table S3. Table S4 shows the count of airway branches, their lengths, and airway volumes among the three groups; no significant differences were found.

Moreover, as *Table 3* shows, the MPAd and MPAd/AAd ratio were more elevated in both the CTED and CTEPH groups than the control group. Pairwise comparisons of these metrics among the three groups are presented in Table S3.

Correlation of pulmonary morphologic parameters with hemodynamics

Figure 5 displays a correlation heat map illustrating the relationships between the pulmonary morphologic parameters, hemodynamics, and clinical indicators. The pulmonary artery tortuosity and bronchovascular bundle tortuosity difference were found to be moderately positively correlated with the mPAP, PVR, and N-terminal-pro-

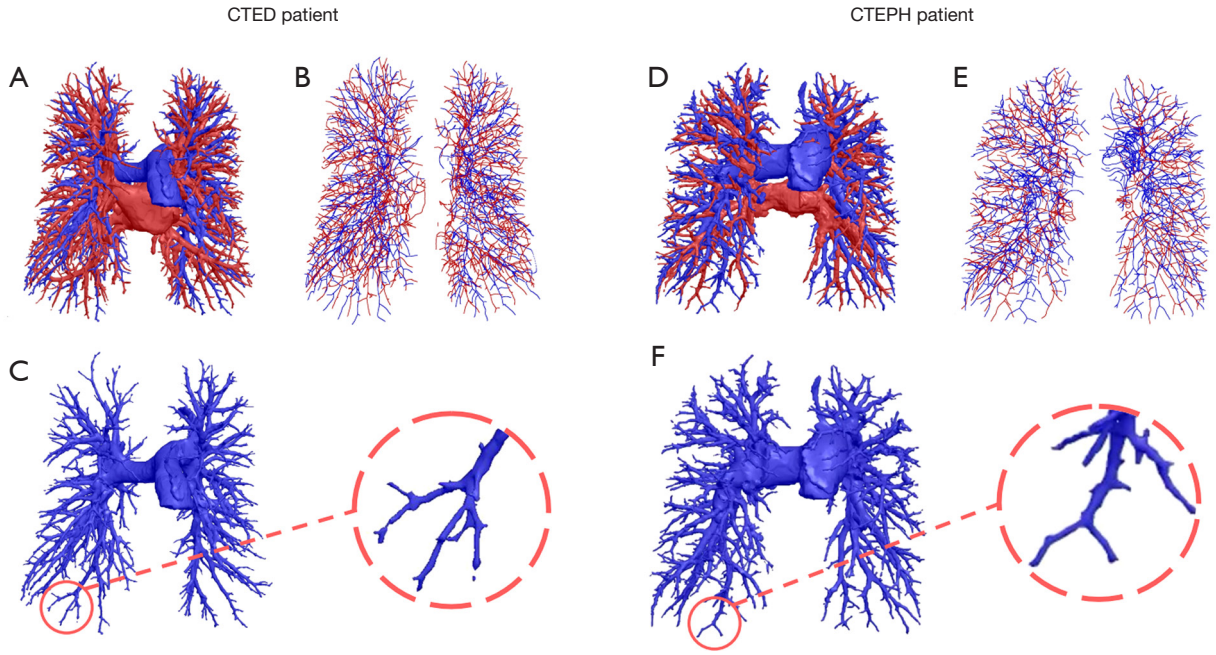

Figure 3 Example of volume reconstruction of pulmonary vessels and vascular tree skeleton in patients. (A-C) Illustrate vascular reconstructions and skeletons of a 56-year-old patient with chronic thromboembolic pulmonary disease; pulmonary arteries are represented in blue, while veins are depicted in red. Notably, the proximal vessels maintain their normal caliber without dilation, and their distal segments exhibit a straight appearance (as indicated by the circle around the A9 segment of the right pulmonary artery). Visually, the venous vascular bed appears denser compared to that typically observed in CTEPH. (D-F) Present vascular reconstructions and skeletons of a 58-year-old patient diagnosed with CTEPH. These images highlight several key features: the proximal pulmonary arteries are notably enlarged; tortuosity is increased (as indicated by the circle around the right A9 segment); and there is evidence of pruning in the distal branches of the pulmonary arteries. CTED, chronic thromboembolic disease; CTEPH, chronic thromboembolic pulmonary hypertension.

Table 2 Comparison of the tortuosity and fractal dimension in the CTEPH, CTED, and control groups

Tortuosity and fractal dimension	Control group (N=20)	CTED group (N=54)	CTEPH group (N=116)	P value[a]
Tortuosity				
Arterial tortuosity	1.07 (1.06–1.10)	1.10 (1.07–1.14)	1.14 (1.10–1.18)	<0.01
Venous tortuosity	1.07 (1.06–1.10)	1.08 (1.06–1.10)	1.08 (1.06–1.10)	0.50
Airway tortuosity	1.02 (1.01–1.02)	1.02 (1.01–1.02)	1.02 (1.01–1.02)	0.58
PA/PV tortuosity ratio	1.00 (0.98–1.03)	1.03 (1.00–1.05)	1.05 (1.01–1.08)	<0.01
Bronchovascular bundle tortuosity difference[b]	0.06 (0.05–0.08)	0.08 (0.06–0.11)	0.12 (0.08–0.16)	<0.01
FD				
Arterial FD	3.02 (2.92–3.07)	3.04 (2.94–3.21)	3.02 (2.93–3.15)	0.36
Venous FD	3.05 (2.92–3.23)	3.06 (2.90–3.20)	3.02 (2.89–3.14)	0.23
Airway FD	3.00 (2.90–3.15)	3.00 (2.84–3.18)	3.04 (2.77–3.24)	0.81

Data are presented as the median and interquartile range for the continuous variables. [a], P value represents two-sided significance from a one-way analysis of variance or Shapiro-Wilks test; [b], the numerical value obtained by subtracting the airway morphological parameters from the pulmonary arterial morphological parameters. CTEPH, chronic thromboembolic pulmonary hypertension; CTED, chronic thromboembolic disease; PA, pulmonary artery; PV, pulmonary vein; FD, fractal dimension.

Table 3 Comparison of CTPA-derived volume metrics among the CTEPH, CTED, and control groups

Volume metrics	Control group (N=20)	CTED group (N=54)	CTEPH group (N=116)	P value[a]
MPAd, mm	24.0 (23.0–26.2)	26.4 (24.5–29.4)	35.6 (32.8–37.9)	<0.01
MPAd/AAd ratio	0.77 (0.67–0.88)	0.84 (0.74–0.98)	1.10 (0.98–1.23)	<0.01
RV/LV ratio	0.78 (0.68–0.89)	0.75 (0.68–0.84)	1.31 (0.95–1.72)	<0.01
Pulmonary artery				
Branch number	1,109 (996–1,234)	880 (766–1,060)	878 (719–1,078)	<0.01
TBV_{ART} (mL)	119.8 (103.2–134.2)	107.1 (88.0–128.7)	123.3 (100.5–142.0)	<0.01
ρBV5 (mL/L)	5.8 (4.8–6.3)	5.4 (4.2–6.2)	4.5 (3.6–5.8)	0.01
ρBV10 (mL/L)	13.4 (10.6–15.7)	13.4 (11.3–15.7)	12.3 (10.2–13.8)	0.04
ρBV10+ (mL/L)	17.0 (12.5–19.6)	15.6 (12.0–20.7)	19.2 (13.7–25.2)	<0.01
$BV5/TBV_{ART}$ (%)	0.19 (0.15–0.23)	0.18 (0.14–0.23)	0.15 (0.10–0.20)	0.03
$BV10/TBV_{ART}$ (%)	0.44 (0.42–0.49)	0.45 (0.38–0.52)	0.40 (0.32–0.45)	<0.01
$BV10+/TBV_{ART}$ (%)	0.55 (0.49–0.57)	0.54 (0.47–0.60)	0.59 (0.53–0.67)	<0.01
Pulmonary vein				
Branch number	1,045 (821–1,100)	880 (745–1,109)	879 (749–1,057)	0.21
TBV_{VEIN} (mL)	121.0 (100.0–133.6)	112.0 (92.8–132.0)	106.0 (88.3–119.5)	0.03
ρBV5 (mL/L)	4.5 (3.8–5.7)	5.3 (3.7–6.1)	4.6 (3.7–5.4)	0.34
ρBV10 (mL/L)	11.8 (10.2–14.2)	13.3 (11.2–15.5)	11.9 (10.3–13.9)	0.20
ρBV10+ (mL/L)	15.4 (12.3–22.3)	19.3 (14.2–24.4)	14.9 (11.4–20.5)	0.05
$BV5/TBV_{VEIN}$ (%)	0.17 (0.14–0.19)	0.16 (0.13–0.19)	0.17 (0.13–0.21)	0.40
$BV10/TBV_{VEIN}$ (%)	0.42 (0.40–0.45)	0.42 (0.39–0.44)	0.44 (0.38–0.48)	0.20
$BV10+/TBV_{VEIN}$ (%)	0.57 (0.53–0.59)	0.57 (0.55–0.61)	0.55 (0.51–0.61)	0.22

Data are presented as the median and interquartile range for the continuous variables. [a], P value represents two-sided significance from a one-way analysis of variance or Shapiro-Wilks test. CTPA, computed tomography pulmonary angiography; CTEPH, chronic thromboembolic pulmonary hypertension; CTED, chronic thromboembolic disease; MPAd, main pulmonary artery diameter; MPAd/AAd ratio, main pulmonary artery to ascending aorta diameter ratio; RV/LV ratio, right ventricle and left ventricle ratio; TBV, total blood volume; TBV_{ART}, total blood volume of pulmonary arteries; TBV_{VEIN}, total blood volume of pulmonary veins.

B-type natriuretic peptide levels (R=0.42–0.47; P<0.01). The BV10+ arteriovenous ratio showed a strong positive correlation with the mPAP and PVR (R=0.66, 0.64; P<0.01). The $BV5/TBV_{ART}$ and $BV10/TBV_{ART}$ ratios were weakly negatively correlated with the mPAP (R=–0.32, –0.39; P<0.01), while the $BV10+/TBV_{ART}$ ratio was weakly positively correlated with the mPAP (R=0.39; P<0.01).

ROC curve analysis

Table 4 presents the diagnostic performance of the pulmonary artery tortuosity and bronchovascular bundle tortuosity difference in distinguishing among the CTEPH, CTED, and control groups. In the comparison of the CTEPH and control groups, pulmonary artery and bronchovascular bundle tortuosity differences greater than 1.12 and 0.07 yielded area under the curve (AUC) values of 0.859 and 0.864 for diagnosing CTEPH (P<0.01). In the comparison of the CTEPH of the CTED groups, tortuosity differences greater than 1.11 and 0.12 yielded AUC values of 0.663 and 0.674 for diagnosing CTEPH (P<0.01). Similarly, in the comparison of the CTED and control groups, tortuosity differences greater than 1.09 and 0.08 yielded AUC values of 0.712 and 0.722 for diagnosing CTED (P<0.01).

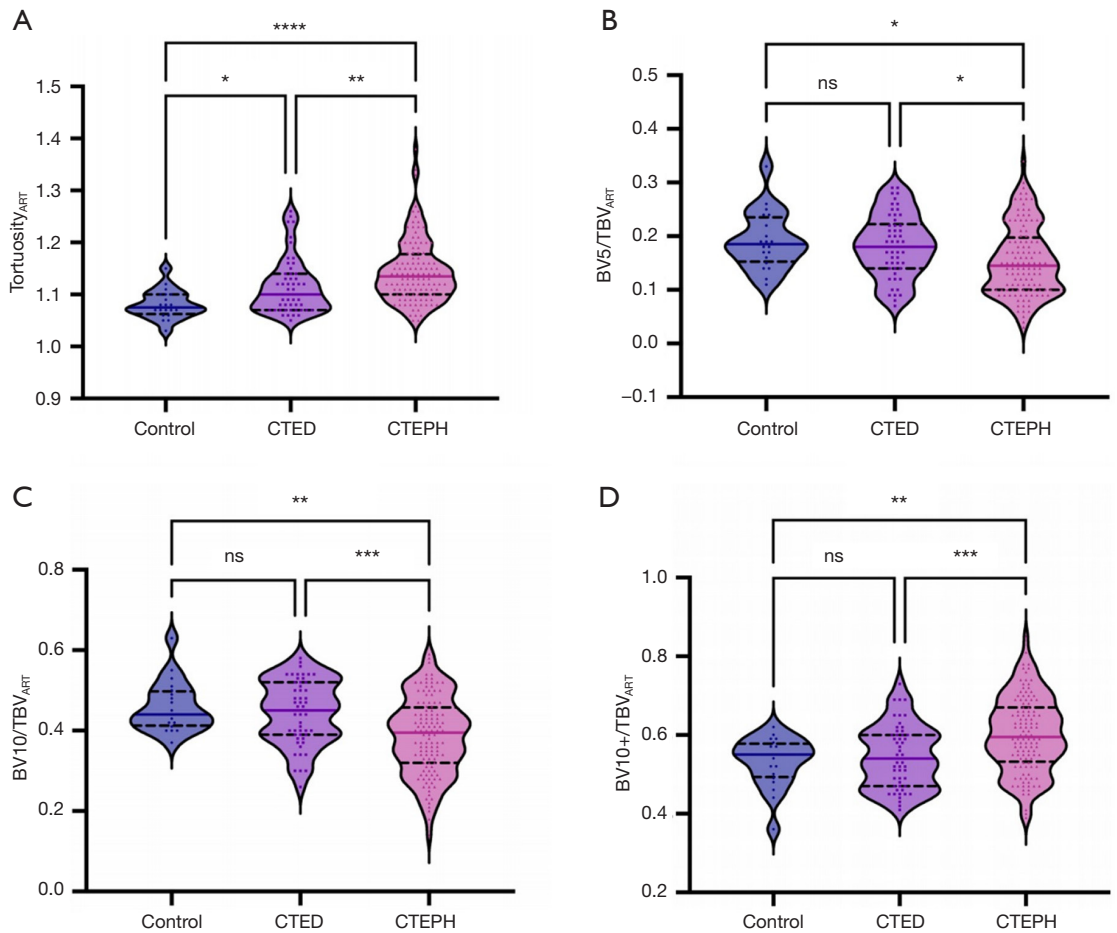

Figure 4 Violin plot of pulmonary artery tortuosity and the pulmonary artery blood volume ratio. The violin plot compares the pulmonary artery tortuosity and proportional volumes of small (BV5), small-to-medium (BV10), and large (BV10+) arteries among the three groups. *, P<0.05; **, P<0.01; ***, P<0.001; ****, P<0.0001; ns, not significant. ART, artery; TBV, total blood volume; CTED, chronic thromboembolic disease; CTEPH, chronic thromboembolic pulmonary hypertension.

Discussion

In this study, we quantitatively analyzed pulmonary vascular tortuosity, FD, and volume on CTPA among CTED, CTEPH, and control groups, and made several notable findings. First, pulmonary artery tortuosity gradually increased across the control, CTED, and CTEPH groups. Second, the FD of pulmonary artery did not change as mPAP and PVR increased. Third, compared to the CTED group, the ρBV5, ρBV10, BV5/TBV$_{ART}$, and BV10/TBV$_{ART}$ parameters were significantly reduced in the CTEPH group.

Following advances in AI for medical imaging and analysis, the automatic segmentation of pulmonary vessels and airway trees has been successfully implemented using an in-house AI workstation (15,16). Tortuosity is a common feature of hypertension in the systemic circulation, where severely twisted vessels can compromise blood flow and lead to ischemia (13,19,20). Similarly, in the pulmonary circulation, as mPAP increases, the pulmonary arteries become progressively more tortuous, reflecting structural changes in response to chronic pressure overload (13,20). We observed a significant increase in pulmonary artery tortuosity in the CTED and CTEPH patients, which aligns with the observations reported by Rahaghi *et al.* (13). Additionally, we found that pulmonary artery tortuosity had a moderate positive correlation with mPAP and PVR; thus, it could serve as an indicator of disease severity in CTED and CTEPH. To our knowledge, the bronchovascular bundle tortuosity difference has not been previously applied in the field of PH. The pulmonary artery tortuosity and

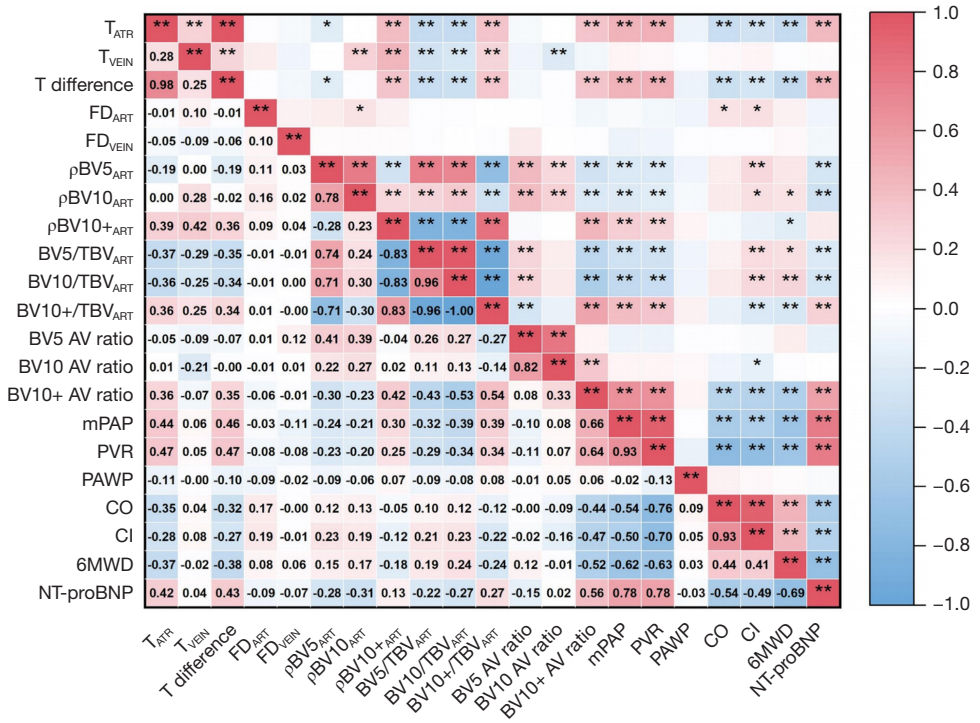

Figure 5 Correlation heatmap of the pulmonary morphological metrics and hemodynamics with clinical indicators. *, P≤0.05; **, P≤0.01. T, tortuosity; ART, artery; T difference, bronchovascular bundle tortuosity difference; FD, fractal dimension; BV, blood volume; TBV, total blood volume; AV, arteriovenous; mPAP, mean pulmonary arterial pressure; PVR, pulmonary vascular resistance; PAWP, pulmonary artery wedge pressure; CO, cardiac output; CI cardiac index; 6MWD, 6-minute walking distance; NT-proBNP, N-terminal-pro-B-type natriuretic peptide.

Table 4 Receiver operating characteristic curves of pulmonary artery-related tortuosity among the CTEPH, CTED, and control groups

Variables	Cut-off value	AUC	SE	95% CI		P value	Sensitivity	Specificity
				Lower limit	Upper limit			
CTEPH *vs.* control group								
Arterial tortuosity	1.12	0.859	0.040	0.786	0.943	<0.01	0.88	0.70
Bronchovascular bundle tortuosity difference	0.07	0.864	0.040	0.780	0.937	<0.01	0.73	0.85
CTEPH *vs.* CTED group								
Arterial tortuosity	1.11	0.663	0.045	0.580	0.758	<0.01	0.73	0.67
Bronchovascular bundle tortuosity difference	0.12	0.674	0.679	0.591	0.767	<0.01	0.51	0.76
CTED *vs.* control group								
Arterial tortuosity	1.09	0.712	0.064	0.588	0.837	<0.01	0.65	0.65
Bronchovascular bundle tortuosity difference	0.08	0.722	0.063	0.598	0.847	<0.01	0.67	0.70

CTEPH, chronic thromboembolic pulmonary hypertension; CTED, chronic thromboembolic disease; AUC, area under the curve; SE, standard error; CI, confidence interval.

bronchovascular bundle tortuosity differences showed substantial diagnostic efficacy in distinguishing between the CTEPH and control groups. However, given the small sample size of the control group, further studies with larger cohorts need to be conducted to validate and confirm these findings. The ability of these tortuosity parameters to differentiate between CTEPH and CTED was not as strong. Additionally, the difference in pulmonary vein tortuosity among the three groups was not statistically significant, which might have been due to factors like the high compliance of the venous system (13).

FD is a metric used to describe irregular or complex shapes (21). Given that both vessels and airways exhibit continuous subdivision and self-similarity, FD can assess the space-filling capacity and structural complexity of vascular and airway trees (19,22-24). A previous study reported that lower FD values in the pulmonary arteries were associated with poorer survival rates (22). Meng *et al.* reported that the pulmonary arterial FD in CTEPH and CTED patients was similar (23). In our study, FD was found to be comparable among the CTEPH, CTED and control groups, and no correlation was found between FD and the hemodynamic parameters.

Following two normalization methods (10,17), the $\rho BV5_{ART}$, $\rho BV10_{ART}$, $BV5/TBV_{ART}$, and $BV10/TBV_{ART}$ parameters, representing small- and medium-sized pulmonary arteries, were significantly reduced in the CTEPH group compared to the CTED and control groups. They also had a weak negative correlation with mPAP. Distal pulmonary microvascular lesions are a key factor in the persistent elevation of mPAP in CTEPH patients (25,26), which suggests that changes in small- and medium-sized pulmonary arteries are important imaging indicators of hemodynamic impairment. These findings align with pathological observations in large animal models of CTEPH, and with changes in CT iodine maps (27). Conversely, $BV5_{ART}$ and $BV10_{ART}$ were significantly higher in the CTED group than the CTEPH group, but were comparable to those in the control group. This is consistent with the finding of Dragsbaek *et al.* (28), who reported no significant distal vessel remodeling in a CTED pig model. Based on these findings, the lack of small-vessel remodeling may explain the absence of PH in CTED. While both the CTEPH and CTED patients had a reduced number of vascular branches compared to the control subjects, the difference between the CTEPH and CTED groups was not statistically significant.

Compared with the CTED and control groups, conventional parameters such as the MPAd, MPAd/AAd ratio, and RV/LV ratio were significantly increased in the CTEPH patients. A previous study indicated that CTED patients may have insignificant right heart dysfunction, especially diastolic dysfunction (29), but these slight functional changes were not reflected in the structural parameters. This suggests that the standardized values of small- and medium-sized pulmonary arteries volume and pulmonary arteries tortuosity are more sensitive indicators than traditional structural parameters, indicating that pulmonary hemodynamic impairment has occurred in CTED patients.

Limitations

The study had several limitations. First, it was a single-center study with a small cohort of CTED patients and control subjects, and the non-normal distribution limits the generalizability of our findings. Larger studies with more diverse populations are needed to validate our results. Second, there is a need to standardize computer algorithms for analyzing the pulmonary vasculature. In this study, we used BV10+ data, which included the BV in the main pulmonary artery, to evaluate pulmonary function and structural changes. Additionally, further refinement in the precision of pulmonary vessel segmentation is necessary, as accurate segmentation is crucial for assessing pulmonary vascular volume reliably.

Conclusions

Pulmonary artery tortuosity has potential as an auxiliary diagnostic tool for distinguishing between CTEPH patients, CTED patients, and control subjects. Additionally, reduced volumes in small- and medium-sized pulmonary arteries may serve as indicators of impaired pulmonary hemodynamics.

Acknowledgments

A portion of this work was presented as a poster at the "European Respiratory Society International Congress 2024" and "The Great Wall International Congress of Cardiology Asian Heart Society Congress 2024".

Footnote

Reporting Checklist: The authors have completed the STROBE reporting checklist. Available at https://qims.

amegroups.com/article/view/10.21037/qims-24-1301/rc

Funding: This study was supported by the National Natural Science Foundation of China (No. 82272081), and the Chinese Academy of Medical Sciences Innovation Fund for Medical Sciences (Nos. 2021-I2M-1-049 and 2022-I2M-C&T-B-109).

Conflicts of Interest: All authors have completed the ICMJE uniform disclosure form (available at https://qims.amegroups.com/article/view/10.21037/qims-24-1301/coif). The authors have no conflicts of interest to declare.

Ethical Statement: The authors are accountable for all aspects of the work in ensuring that questions related to the accuracy or integrity of any part of the work are appropriately investigated and resolved. The study was conducted in accordance with the Declaration of Helsinki (as revised in 2013) and was approved by the China-Japan Friendship Hospital's Ethics Committee (No. 2022-KY-048). The requirement of informed consent was waived due to the retrospective nature of the study.

References

1. Lang IM, Campean IA, Sadushi-Kolici R, Badr-Eslam R, Gerges C, Skoro-Sajer N. Chronic Thromboembolic Disease and Chronic Thromboembolic Pulmonary Hypertension. Clin Chest Med 2021;42:81-90.
2. Reddy SA, Swietlik EM, Robertson L, Michael A, Boyle S, Polwarth G, Screaton NJ, Ruggiero A, Nethercott SL, Taboada D, Sheares KK, Hadinnapola C, Cannon JE, Bunclark K, Jenkins D, Ng C, Toshner MR, Pepke-Zaba J. Natural history of chronic thromboembolic pulmonary disease with no or mild pulmonary hypertension. J Heart Lung Transplant 2023;42:1275-85.
3. Luijten D, Talerico R, Barco S, Cannegieter SC, Delcroix M, Ende-Verhaar YM, Huisman MV, Konstantinidis S, Mairuhu ATA, van Mens TE, Ninaber M, Pruszczyk P, Vonk Noordegraaf A, Klok FA. Incidence of chronic thromboembolic pulmonary hypertension after acute pulmonary embolism: an updated systematic review and meta-analysis. Eur Respir J 2023;62:2300449.
4. Humbert M, Kovacs G, Hoeper MM, Badagliacca R, Berger RMF, Brida M, et al. 2022 ESC/ERS Guidelines for the diagnosis and treatment of pulmonary hypertension. Eur Respir J 2023;61:2200879.
5. Delcroix M, de Perrot M, Jaïs X, Jenkins DP, Lang IM, Matsubara H, Meijboom LJ, Quarck R, Simonneau G, Wiedenroth CB, Kim NH. Chronic thromboembolic pulmonary hypertension: realising the potential of multimodal management. Lancet Respir Med 2023;11:836-50.
6. Stam K, Clauss S, Taverne YJHJ, Merkus D. Chronic Thromboembolic Pulmonary Hypertension - What Have We Learned From Large Animal Models. Front Cardiovasc Med 2021;8:574360.
7. Konstantinides SV, Meyer G, Becattini C, Bueno H, Geersing GJ, Harjola VP, et al. 2019 ESC Guidelines for the diagnosis and management of acute pulmonary embolism developed in collaboration with the European Respiratory Society (ERS). Eur Heart J 2020;41:543-603.
8. McQuade C, Grafham G, Donahoe L, Granton J, De Perrot M, McInnis M. Comparison of CT Scoring in Chronic Thromboembolic Pulmonary Disease (CTED) versus Chronic Thromboembolic Pulmonary Hypertension (CTEPH). The Journal of Heart and Lung Transplantation 2024;43:S449.
9. Pu J, Leader JK, Sechrist J, Beeche CA, Singh JP, Ocak IK, Risbano MG. Automated identification of pulmonary arteries and veins depicted in non-contrast chest CT scans. Med Image Anal 2022;77:102367.
10. Rahaghi FN, Nardelli P, Harder E, Singh I, Sánchez-Ferrero GV, Ross JC, San José Estépar R, Ash SY, Hunsaker AR, Maron BA, Leopold JA, Waxman AB, San José Estépar R, Washko GR. Quantification of Arterial and Venous Morphologic Markers in Pulmonary Arterial Hypertension Using CT Imaging. Chest 2021;160:2220-31.
11. Cheung WK, Pakzad A, Mogulkoc N, Needleman S, Rangelov B, Gudmundsson E, Zhao A, Abbas M, McLaverty D, Asimakopoulos D, Chapman R, Savas R, Janes SM, Hu Y, Alexander DC, Hurst JR, Jacob J. Automated airway quantification associates with mortality in idiopathic pulmonary fibrosis. Eur Radiol 2023;33:8228-38.

12. Tanabe N, Sato S, Suki B, Hirai T. Fractal Analysis of Lung Structure in Chronic Obstructive Pulmonary Disease. Front Physiol 2020;11:603197.
13. Rahaghi FN, Ross JC, Agarwal M, González G, Come CE, Diaz AA, Vegas-Sánchez-Ferrero G, Hunsaker A, San José Estépar R, Waxman AB, Washko GR. Pulmonary vascular morphology as an imaging biomarker in chronic thromboembolic pulmonary hypertension. Pulm Circ 2016;6:70-81.
14. Sun H, Liu M, Kang H, Yang X, Zhang P, Zhang R, Dai H, Wang C. Idiopathic pulmonary fibrosis disease progression: a dynamic quantitative chest computed tomography follow-up analysis. Quant Imaging Med Surg 2023;13:1488-98.
15. Sun X, Meng X, Zhang P, Wang L, Ren Y, Xu G, Yang T, Liu M. Quantification of pulmonary vessel volumes on low-dose computed tomography in a healthy male Chinese population: the effects of aging and smoking. Quant Imaging Med Surg 2022;12:406-16.
16. Huang X, Yin W, Shen M, Wang X, Ren T, Wang L, Liu M, Guo Y. Contributions of Emphysema and Functional Small Airway Disease on Intrapulmonary Vascular Volume in COPD. Int J Chron Obstruct Pulmon Dis 2022;17:1951-61.
17. Rahaghi FN, Hilton JF, Corrêa RA, Loureiro C, Ota-Arakaki JS, Verrastro CGY, Lee MH, Mickael C, Nardelli P, Systrom DA, Waxman AB, Washko GR, San José Estépar R, Graham BB, Oliveira RKF. Arterial vascular volume changes with haemodynamics in schistosomiasis-associated pulmonary arterial hypertension. Eur Respir J 2021;57:2003914.
18. Maron BA, Kovacs G, Vaidya A, Bhatt DL, Nishimura RA, Mak S, Guazzi M, Tedford RJ. Cardiopulmonary Hemodynamics in Pulmonary Hypertension and Heart Failure: JACC Review Topic of the Week. J Am Coll Cardiol 2020;76:2671-81.
19. Helmberger M, Pienn M, Urschler M, Kullnig P, Stollberger R, Kovacs G, Olschewski A, Olschewski H, Bálint Z. Quantification of tortuosity and fractal dimension of the lung vessels in pulmonary hypertension patients. PLoS One 2014;9:e87515.
20. Bullitt E, Gerig G, Pizer SM, Lin W, Aylward SR. Measuring tortuosity of the intracerebral vasculature from MRA images. IEEE Trans Med Imaging 2003;22:1163-71.
21. Lopes R, Betrouni N. Fractal and multifractal analysis: a review. Med Image Anal 2009;13:634-49.
22. Haitao S, Ning L, Lijun G, Fei G, Cheng L. Fractal dimension analysis of MDCT images for quantifying the morphological changes of the pulmonary artery tree in patients with pulmonary hypertension. Korean J Radiol 2011;12:289-96.
23. Meng XP, Sun XB, Xu WQ, Tao XC, Xie WM, Liu M. Comparison of pulmonary vascular tortuosity and fractal dimension in patients with chronic thromboembolic pulmonary disease and chronic thromboembolic pulmonary hypertension. Zhonghua Jie He He Hu Xi Za Zhi 2023;46:774-80.
24. Moledina S, de Bruyn A, Schievano S, Owens CM, Young C, Haworth SG, Taylor AM, Schulze-Neick I, Muthurangu V. Fractal branching quantifies vascular changes and predicts survival in pulmonary hypertension: a proof of principle study. Heart 2011;97:1245-9.
25. Lang IM, Madani M. Update on chronic thromboembolic pulmonary hypertension. Circulation 2014;130:508-18.
26. Ukita R, Tipograf Y, Tumen A, Donocoff R, Stokes JW, Foley NM, Talackine J, Cardwell NL, Rosenzweig EB, Cook KE, Bacchetta M. Left Pulmonary Artery Ligation and Chronic Pulmonary Artery Banding Model for Inducing Right Ventricular-Pulmonary Hypertension in Sheep. ASAIO J 2021;67:e44-8.
27. Tang CX, Yang GF, Schoepf UJ, Han ZH, Qi L, Zhao YE, Wu J, Zhou CS, Zhu H, Stubenrauch AC, Mangold S, Zhang LJ, Lu GM. Chronic thromboembolic pulmonary hypertension: Comparison of dual-energy computed tomography and single photon emission computed tomography in canines. Eur J Radiol 2016;85:498-506.
28. Dragsbaek SJ, Lyhne MD, Hansen JV, Pedersen CCE, Jujo-Sanada T, Karout L, Kalra MK, Nielsen-Kudsk JE, Andersen A. A porcine model of human-like chronic thromboembolic pulmonary disease. Thromb Res 2023;231:25-8.
29. McCabe C, White PA, Hoole SP, Axell RG, Priest AN, Gopalan D, Taboada D, MacKenzie Ross R, Morrell NW, Shapiro LM, Pepke-Zaba J. Right ventricular dysfunction in chronic thromboembolic obstruction of the pulmonary artery: a pressure-volume study using the conductance catheter. J Appl Physiol (1985) 2014;116:355-63.

Cite this article as: Xu W, Xi L, Ni Y, Wang J, Yang H, Liu A, Gao Q, Tao X, Huang Q, Liu X, Zhen Y, Xie W, Liu M. Artificial intelligence-driven quantitative analysis of CT morphological differences between chronic thromboembolic pulmonary hypertension and chronic thromboembolic disease. Quant Imaging Med Surg 2025;15(2):1101-1113. doi: 10.21037/qims-24-1301

